Journal of Radiological Science and Technology, 41(2), 141-148 ISSN 2384-1168(On-line) ISSN 2288-3509(Print)

<원저>

전신방사선조사 시 선속 스포일러에 따른 선량 분포 및 영향 평가

이동연[1)]·김정훈[2)]

[1)]동남권원자력의학원 방사선종양학과·[2)]부산가톨릭대학교 방사선학과

Beam Spoiler-dependent Total Body Irradiation Dose Assessment

Dong-Yeon Lee[1)]·Jung-Hoon Kim[2)]

[1)]*Department of Radiation Oncology, Dongnam Institute of Radiological & Medical Science*

[2)]*Department of Radiology, Catholic University of Pusan*

Abstract This study examined the properties of photons and the dose distribution in a human body via a simulation where the total body irradiation(TBI) is performed on a pediatric anthropomorphic phantom and a child size water phantom. Based on this, we tried to find the optimal photon beam energy and material for beam spoiler. In this study, MCNPX (Ver. 2.5.0), a simulation program based on the Monte Carlo method, was used for the photon beam analysis and TBI simulation. Several different beam spoiler materials (plexiglass, copper, lead, aluminium) were used, and three different electron beam energies were used in the simulated accelerator to produce photon beams (6, 10, and 15 MeV). Moreover, both a water phantom for calculating the depth-dependent dosage and a pediatric anthropomorphic phantom for calculating the organ dosage were used. The homogeneity of photon beam was examined in different depths for the water phantom, which shows the 20%-40% difference for each material. Next, the organ doses on pediatric anthropomorphic phantom were examined, and the results showed that the average dose for each part of the body was skin 17.7 Gy, sexual gland 15.2 Gy, digestion 13.8 Gy, liver 11.8 Gy, kidney 9.2 Gy, lungs 6.2 Gy, and brain 4.6 Gy. Moreover, as for the organ doses according to materials, the highest dose was observed in lead while the lowest was observed in plexiglass. Plexiglass in current use is considered the most suitable material, and a 6 or 10 MV photon energy plan tailored to the patient condition is considered more suitable than a higher energy plan.

Key Words: Leukaemia, Total body irradiation, Beam spoiler, MCNPX, Dose assessment

중심 단어: 백혈병, 전신방사선조사, 빔 스포일러, MCNPX, 선량평가

Ⅰ. INTRODUCTION

Leukaemia, which makes up ~30% of all childhood cancers[1], is characterized by malignant transformation of hematopoietic cells followed by proliferation within bone marrow and lymph nodes and subsequent release into peripheral blood and infiltration into various tissues[2]. Chemotherapy and hematopoietic stem cell transplantation (HSCT) are its standard therapies[2], employed for low- and high-risk patient groups, respectively[3]. In particular, HSCT is preferred in pediatric patients as a curative therapy[4].

Pre-treatment, an integral part of HSCT, fulfils two important functions: removing cancerous cells that may remain in the existing hematopoietic cells, and preparing a favourable condition for the engraftment of the transplanted hematopoietic stem cells by providing sufficient immunosuppression of

Corresponding author: Kim Jung Hoon, Department of Radiology, Catholic University of Pusan, 57 Oryundae-ro, Geumjeong-gu, Busan, 46252, Korea / Tel : +82-51-510-0589 / E-mail: donald@cup.ac.kr
Received 27 February 2018; Revised 27 March 2018; Accepted 21 April 2018

the existing hematopoietic cells[5,6].

Total body irradiation (TBI) and chemotherapy are used as preparatory regimens either alone or in combination[7]. TBI is easy to administer and has other advantages over chemotherapeutic agents, such as cost-effectiveness and absence of cross-tolerance to other anticancer agents. In addition, it ensures uniform irradiation of the entire body irrespective of the blood flow rate, thus reaching the tissues and organs difficult to penetrate with anticancer agents[7]. However, TBI can have adverse outcomes such as growth retardation, developmental disorders, hormonal imbalance, neurological complications, and secondary malignancies[8]. Pre-intervention dose assessment for each organ is especially important for children because they are considerably more sensitive to radiation than adults are. Currently, the dose-related recommendation for TBI only states that over 90% of prescribed dose should be absorbed into the skin surface without any mention of internal organ doses [4-6,8-9].

In this study, we examined the properties of photons and the dose distribution in a human body via a simulation where the total body irradiation is performed on a pediatric anthropomorphic phantom and a child size water phantom. Based on this, we tried to find the optimal photon beam energy and material for beam spoiler. Therefore, a simulation with water phantom and pediatric anthropomorphic phantom in virtual space is conducted to examine the doses on human organs using the pediatric anthropomorphic phantom and the properties of photons according to water depths. Based on this, we aim to determine whether the existing plexiglass material currently used for the TBI can be replaced and to propose the optimal photon beam energy.

II. MATERIALS AND METHODS

MCNPX, as a code using the Monte-Carlo method, was developed by Los Alamos National Laboratory. It can transport a total of 34 particles including electron, photon, neutron, and quantum while defining various types of desired calculations and source terms for users[10]. Moreover, MCNPX runs under Windows operating systems, which makes the code accessible for users. In particular, the Tally, as a code that represents a way of expressing the resulting values, allows different physical quantity such as fluency, energy distribution, or energy absorption to be printed out. The tallies used for this research are F5 and F6. F5 is used to represent the number of particles per unit area (㎠) with an imaginary spherical detector installed in a desired space. F6 expresses the energy (MeV) received per unit mass (g) by specifying a region of interest. MCNPX was used for evaluating the dose, and the resulting values were calculated in MeV/g by using Tally 6, which were converted into units of Gy. The calculation was performed assuming that 16 Gy is prescribed in the AP direction since the dose allowed for total body irradiation is usually 32 Gy.

In this study, MCNPX (Ver. 2.5.0)[10], a simulation program based on the Monte Carlo method, was used for photon beam analysis and TBI simulation. First, photons generated by a simulated linear accelerator head were analysed, and TBI was performed on a simulated real-size water phantom and pediatric anthropomorphic phantom for dose assessment for different water depths and various organs.

1. Photon beam spectra

The simulation in this study was built on the basis of the shape and material of a linear accelerator borrowed from existing research studies, rather than using a linear accelerator produced by a specific company, in order to obtain standardized data[11-12]. In line with the analysis purpose, i.e. observations of beam patterns and dose distributions on the water phantom and the pediatric anthropomorphic phantom exposed to TBI, respectively, a simplified linear accelerator structure was used for simulation purposes focusing on the linear accelerator head where photons are generated. Fig. 1 shows the geometric structure of the linear accelerator head. The beam energy for the dose assessment was varied between 6, 10, and 15

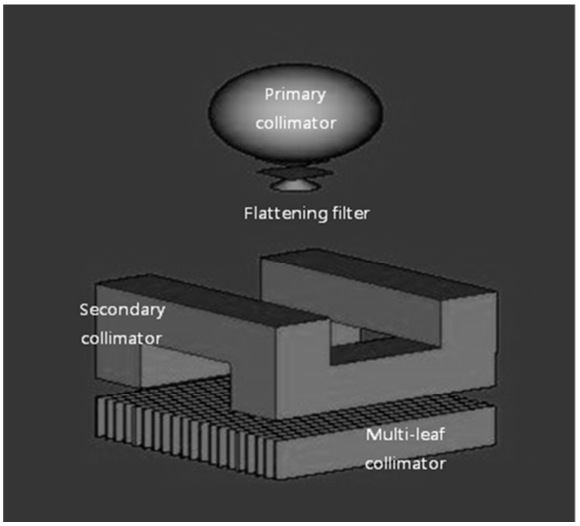

Fig. 1 Schematic of the linear accelerator head in MCNPX

MeV, and a round virtual dosimeter was placed under the 10 ㎝ point immediately after the flattening filter, making calculates at 1 keV intervals. The F5 tally option was used, and the photon flux per electron was expressed as the number of incident photons per unit area (㎠) per second. The reliability of the simulated linear accelerator head was evaluated on the basis of the photon spectra calculated, and the TBI-related dose assessment was performed using the water phantom and the pediatric anthropomorphic phantom.

2. Water phantom

The simulated real-size water phantom model was based on an average 5-year-old child (height: 110 ㎝, weight: 18 ㎏, thickness: 15 ㎝), the age with the highest leukaemia incidence[13-15]. The thickness was partitioned at 1 ㎝ interval to enable thickness-dependent dose assessment (Fig. 2). The F6 tally option was used for calculating the total energy deposition within a 1 cm slice. The deposited energy (MeV/g) calculated was then converted into absorbed dose (Gy).

3. Pediatric anthropomorphic phantom

The pediatric anthropomorphic phantom used in this study is the UF Revised ORNL phantom for pediatric radiology, a medical internal radiation dose

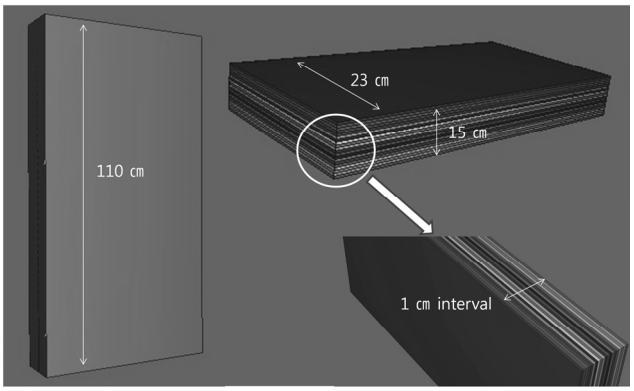

Fig. 2 Water phantom similar to pediatric

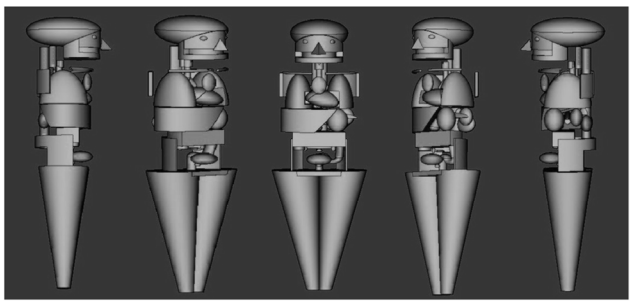

Fig. 3 Images of the anthropomorphic phantom in anterior, diagonal, and lateral position

(MIRD)-type phantom. The UF Revised ORNL phantom is a revised version of the whole-body anthropomorphic phantom developed at the Oak Ridge National Laboratory (ORNL) for calculating internal radiation exposure of the organs made of specific materials. The revised ORNL phantom includes the head (containing the brain), kidneys, recto-sigmoid colon, and extrapulmonary airway based on a recently developed anthropomorphic model, in addition to salivary glands, bladder mucosa, a digestive tract, and airway. Fig. 3 schematically illustrates the organs[13] with their respective masses and densities in accordance with the specifications of the International Commission on Radiological Protection (ICRP) 89[14] and International Commission on Radiation Units and Measurements (ICRU) 46[15]. The F6 tally option was used for calculating the deposited energy (MeV/g), which were then converted into the absorbed dose (Gy). The elemental composition, percentage, density, and volume for materials that make up brain, lung, skin, muscle, liver, kidney, genital gland, and digestion are shown in Tables 1 and 2.

Table 1 Composition of the tissue for the anthropomorphic phantom.

Element	Percent by weight								
	Brain	Lung	Liver	Digestion	Skin	Muscle	Testis	Ovary	Kidney
H	10.7	10.3	10.3	10.6	10	10.2	10.6	10.5	10.3
C	14.5	10.5	18.6	11.5	20.4	14.3	9.9	9.3	13.2
N	2.2	3.1	2.8	2.2	4.2	43.4	2.0	2.4	3.0
O	71.2	74.9	67.1	75.1	64.5	71	76.6	76.8	72.4
Na	0.2	0.2	0.2	0.1	0.2	0.1	0.2	0.2	0.2
P	0.4	0.2	0.2	0.1	0.1	0.2	0.1	0.2	0.1
S	0.2	0.3	0.3	0.1	0.2	0.3	0.2	0.2	
Cl	0.3	0.3	0.2	0.2	0.3	0.1	0.2	0.2	
Ka	0.3	0.2	0.3	0.1	0.1	0.4	0.2	0.2	
Mg									0.2
Si									0.2

Table 2 Volume and density of anthropomorphic Phantom

Organ	Density (g/cm^3)	Volume (cm^3)	Organ	Density (g/cm^3)	Volume (cm^3)
Brain	1.04	1194	Lung	0.260	980
Digestion	1.03	439.14	Liver	1.05	562
Skin	1.09	514.74	Muscle	1.03	7547.568
Ovary	1.05	1.66	Testis	1.04	1.57
Kidney	1.05	111.12			

4. Materials for beam spoiler

Materials used for the beam spoiler were 1.5 ㎝ plexiglass ($C_5O_2H_8$, density:1.16 g/㎤)[16] widely used in clinical settings as a reference material, 1.5 cm aluminium (^{13}Al, density: 2.7 g/㎤, Al) with similar atomic number and density, and 0.3 cm copper (^{29}Cu, density: 8.94 g/㎤, Cu) and lead (^{82}Pb, density: 11.34 g/㎤, Pb) with higher atomic numbers and densities. The thicknesses were calculated on the basis of previous studies[17-18], which indicated similar doses were yielded when the thickness of the Cu was about one third the thickness of the Al material. While existing theories recommend the closest possible beam spoiler-to-patient distance (SPD)[4-7], SPD was set at 10 cm, given that gapless application is not implementable. Furthermore, as materials for the head and lungs requiring shielding, we used Lipowitz alloy (^{83}Bi, ^{82}Pb, ^{50}Sn, ^{48}Cd, density: 9.4 g/㎤), which has a high shielding rate and low melting point due to the high atomic numbers of the components, and ensured sufficient shielding with a thickness of 7.5 ㎝ corresponding to 5 half value layers that can shield ≥ 95% of the primary beam[6].

5. Simulation methods

Of the two major TBI methods, we used the anterior-posterior method in which radiation is delivered towards the body front with the umbilicus as the midpoint[9]. Photon energy intensity was varied to 6, 10, and 15 MV in the continuous radiation beams analysed in this study, and the source-to-skin distance (SSD) was set at 300 cm to sufficiently cover the height of 110 cm. Simulations were performed as described below and the depth-dependent doses and organ doses were calculated and evaluated in the water phantom and anthropomorphic phantom, respectively. The simulation values were converted on the basis of the assumption that TBI is administered at 16 Gy.

Ⅲ. RESULTS

1. Photon spectra

Fig. 4 illustrates the photon beam spectra obtained using electron beams of 6, 10, and 15 MeV in a simulated linear accelerator. The average energies for the calculated photons were 1.44, 2.12, and 2.85 MeV at 6, 10, and 15 MeV incident energies, respectively, and the incident photon energy of 511 keV was calculated for all variants.

2. Thickness-dependent dose calculated in the water phantom

Fig. 5 shows the absorbed dose (Gy) versus the thickness of the water phantom at 1-cm intervals.

Dosimetric comparison between the incident photon beam area (1 ㎝) and the deepest area (15 ㎝) revealed the average dose differences for Al, plexiglass, Cu, and Pb to be 40.2%, 40.9%, 35.5%, and 21%, respectively, showing similar energy-dependent dose differences.

3. Deep organ dose

In the following, Fig. 6 shows radiation simulations of deep organ dose in terms of the absorbed dose (Gy) in the skin, sexual gland, digestive tract, liver, kidneys, lungs, and brain. The approximate average absorbed dose and energy- and material-dependent changes in dose for each organ are as follows.

Skin: 17.7 Gy; in plexiglass, Al, and Cu, the dose was inversely related to energy, and in Pb, positively related.

Sexual gland: 15.2 Gy; a lower dose was observed for 10 MV compared to 6 and 15 MV.

Digestive track: 13.8 Gy; in plexiglass, Al, and Cu, the dose was inversely related to energy, and in Pb, it was positively related.

Liver: 11.8 Gy; in plexiglass, the dose was inversely related to energy, and the highest dose was recorded at 6 MV in Al and Cu, and at 15 MV in Pb.

Kidneys: 9.2 Gy; in plexiglass, Al and Cu, the highest dose was recorded at 6 MV, and in Pb, at 15 MV.

Lungs: 6.2 Gy, in plexiglass, Al, and Cu, the dose was inversely related to energy, and in Pb, a slightly higher dose was exhibited at 10 MV compared to other doses.

Brain: 4.6 Gy; in plexiglass, Al, and Cu, the dose was inversely related to energy, and in Pb, the highest dose was exhibited at 6 MV.

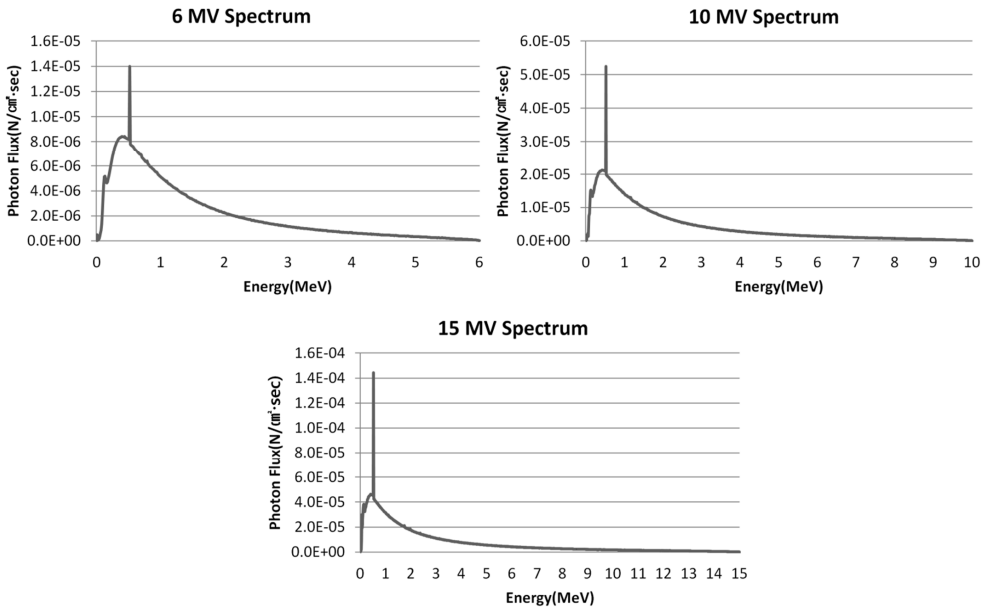

Fig. 4 Photon spectra calculated in the simulation

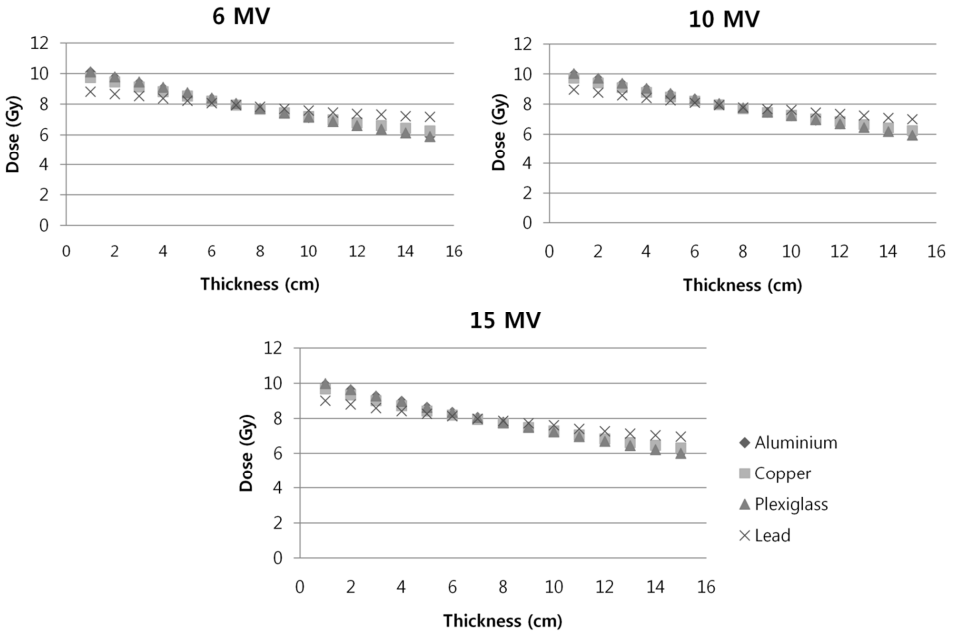

Fig. 5 Thickness-dependent doses calculated in the water phantom

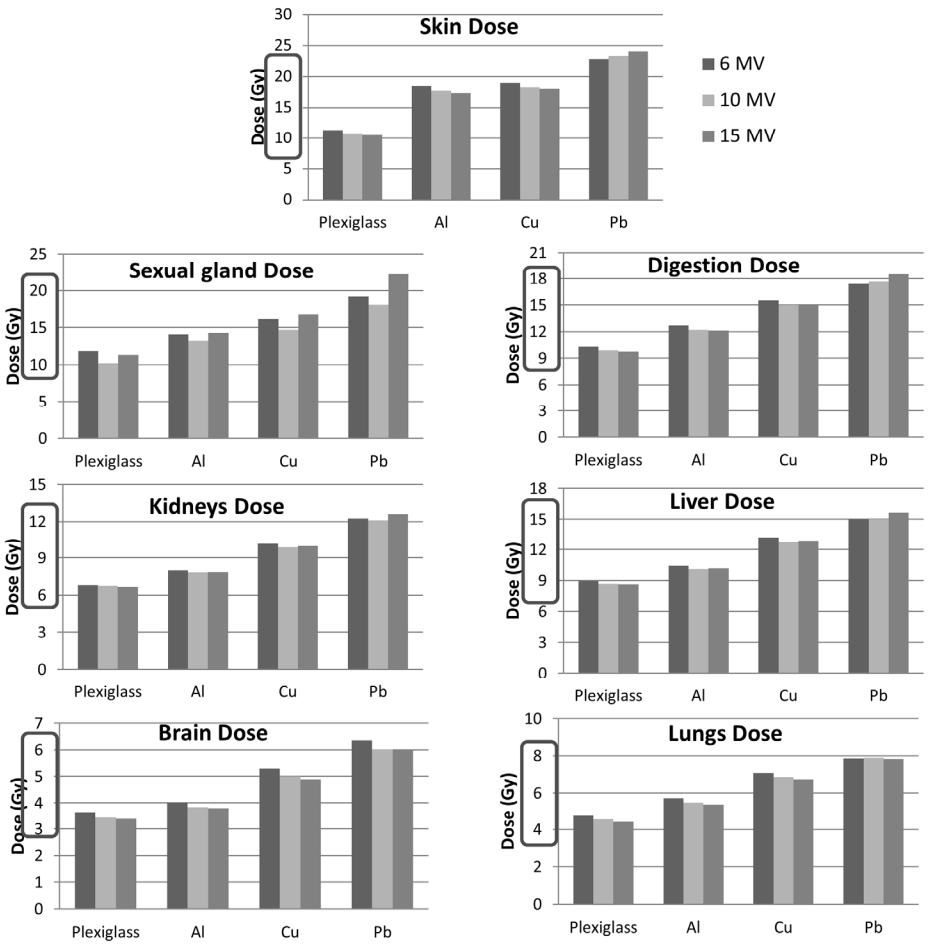

Fig. 6 Material- and energy-dependent deep organ doses

Ⅳ. DISCUSSION

This study carried out a simulation on water phantom and pediatric anthropomorphic phantom to examine the effects of the total body irradiation on children.

First, the average photon beam energy at 6 MV calculated in this study was ~10% lower than those calculated by Mesbahi et al.[19] using Geant3 and by Baumgartner et al.[20] using PENELOPE-2006 (1.67 and 1.65 MeV, respectively). This is assumed to be attributable to the geometric difference of the linear accelerator simulated in this study and the point of calculate of the photon spectra, especially the calculate point placement underneath the target where low-energy photons are concentrated.

Second, the depth-dependent dose in the water phantom showed smaller differences between the shallowest (1 ㎝) and deepest (15 ㎝) positions when Cu and Pb materials were used as the beam spoiler compared to the plexiglass or Al materials, with the Pb material showing the smallest dose difference. This may be explained by the high absorption rate of low-energy photons in a high atomic number and high density material, resulting in beam hardening.

Third, the organ doses were calculated on the pediatric anthropomorphic phantom in the decreasing order of skin, sexual gland, digestive, liver, kidneys, lungs, and brain. Such differences may be ascribed to the differences in volume and density of the organs. The low organ doses for the lungs and brain are attributable to the shielding calculate, and for the kidneys, to their position in the retroperitoneal space and thus lower exposure to the anterior-posterior delivered radiation.

Fourth, the material-dependent dose showed the highest value by plexiglass, followed by Al, Cu, and Pb. This is because material with a high atomic number and high density absorbs a higher amount of photons. Therefore, high organ doses may be ascribed to the necessity for corresponding dose adjustments to ensure sufficient prescribed doses.

Ⅴ. CONCLUSION

This study aims to determine whether the plexiglass beam spoiler currently used in clinical settings during the total body irradiation can be replaced with other materials such as Al, Cu, or Pb, and to propose an optimal photon beam energy.

First, Pb and Cu are not suitable materials because they incur high organ doses by absorbing large amount of photons, but they are advantageous in terms of depth-dependent beam homogeneity.

Second, energy and organ dose are inversely related. However, 15 MV is considered unsuitable because it does not satisfy the requirement for more than 90% of the prescribed dose.

Lastly, taking these analysis results together, Plexiglass in current use is considered the most suitable material, and a 6 or 10 MV photon energy plan tailored to patient condition is considered more suitable than a higher energy plan.

REFERENCES

[1] Kim SH. Identification of symptoms by treatment phases in children with leukemia. [Master's thesis]. Seoul: Graduate School of Nursing Yonsei University; 2009.

[2] Park YK. The impacts of the in-patient' copayment waiver policy on medical services and outcomes for leukemia children. [Master's thesis], Seoul: Graduate School of Public Health Yonsei University; 2008.

[3] Kim SR, Kim HJ, Kim SH. Clinical utility of fluo-rescence in-situ hybridization profile test in detect-ing genetic aberrations in acute leukemia. Korean J Lab Med. 2009;29:371-378.

[4] Beaumais TA, Fakhoury M, Medard Y, Azougagh S, Zhang D, Yakouben K, et al. Determinants of mer-captopurine toxicity in paediatric acute lympho-blastic leukemia maintenance therapy. British Journal of clinical Pharmacology. 2010;71(4): 575-584.

[5] Van Dyk J, Galvin JM, Glasgow GP, Podgorsak EB.. AAPM REPORT NO. 17: The Physical Aspects of Total

and Half Body Photon Irradiation. New York: Radiation Therapy Committee American Association of Physics in Medicine; 1986.

[6] Thomas ED, Buckner CD, Banaji M, Clift RA, Fefer A, Flournoy N, et al. One hundred patients with acute leukemia treated by chemotherapy, total body irradiation, and allogeneic marrow transplantation. Blood J. 1977;49(4):511-533.

[7] Kim SJ, Han DK, Baek HJ, Kim DY, Nam TK, Hwang TJ, et al. Comparison of total body irradiation-based or non-total body irradiation-based conditioning regimens for allogeneic stem cell transplantation in pediatric leukemia patients. Korean J Pediat. 2010;53(4):538-547.

[8] Perez CA, Brady LW, Halperin EC, Wazer DE. Principles and Practice of Radiation Oncology. 4th ed. New York: Lippincott Williams & Wilkins; 2004.

[9] Aristei C, Tabilio A. Total-body irradiation in the conditioning regimens for autologous stem cell transplantation in lymphoproliferative diseases. The oncologist. 1999;4:386-397.

[10] Denis B. Pelowits. MCNPX^{TM} User's manual version2.5.0 .LosAlamos National Laboratory, 2005.

[11] Lin JP, Liu WC, Lin CC. Investigation of photo-neutron dose equivalent from high-energy photons in radiotherapy. Applied Radiation and Isotopes. 2007;65:599-604.

[12] Huang WL, Li QF, Lin TZ. Calculation of photo-neutrons produced in the targets of electron linear accelerators for radiography and radiotherapy applications. Nucl Instr and Meth in Phy Res. 2005;B229:339-347.

[13] Han EY, Bolch WE, Eckerman KF. Revision to the ORNL series of adult and pediatric computational phantoms for use with the MIRD schema. Health Phys. 2006;90:337-356.

[14] Valentin J. ICRP 89: Basic Anatomical and Physiological Data for Use in Radiological Protection Reference Values. Internatioal Commission on Radiological Protection; 2002.

[15] White DR, Griffith RV, Wilson IJ. ICRU Report 46: Photon, electron, proton and neutron interaction data for body tissues. Internatioal Commission on Radiation Units and Measurements; 1992.

[16] Choi JH, Kim JS, Choi JM Shin EH, Song KW, Park YH. Analysis of surface dose refer to distance between beam spoiler and patient in total body irradiation. J Korea Soc Ther Radiol. 2007;19(1):51-54.

[17] Lee MY. The effect of x-ray filter materials in the skin dose & tube loading at x-ray examinations. [Master's thesis]. Seoul: Dept. of Health Science Graduate School Korea University; 2005.

[18] Ravichandran R, Binukumar JP, Davis CA, Sivakumar SS, Krishnamurthy K, Mandhari ZA, et al. Beam configuration and physical parameters of clinical high energy photon beam for total body irradiation (TBI). Phys Med. 2011;27:163-168.

[19] Mesbahi A, Fix M, Allahverdi M, Grein E, Garaati H. Monte Carlo calculation of Varian 2300C/D Linac photon beam characteristics: a comparison between MCNP4C, GEANT3 and measurements. Appl Radiat Isotopes 2005;62(3):469-477.

[20] Baumgartner A, Steurer A, Maringer F. Simulation of photon energy spectra from Varian 2100C and 2300C/D Linacs: Simplified estimates with PENELOPE Monte Carlo models. Appl Radiat Isotopes. 2009;67(11):2007-2012.

[21] Clare Mckay, Kellie A, Caroline Wright. Beyond cancer treatment - a review of total lymphoid irradiation for heart and lung transplant recipients. Journal of medical radiation science. 2014;61:202-209.